

Estimation of Faults in DC Electrical Power System

Dimitry Gorinevsky, Stephen Boyd, and Scott Poll,

Abstract—This paper demonstrates a novel optimization-based approach to estimating fault states in a DC power system. Potential faults changing the circuit topology are included along with faulty measurements. Our approach can be considered as a relaxation of the mixed estimation problem. We develop a linear model of the circuit and pose a convex problem for estimating the faults and other hidden states. A sparse fault vector solution is computed by using l_1 regularization. The solution is computed reliably and efficiently, and gives accurate diagnostics on the faults. We demonstrate a real-time implementation of the approach for an instrumented electrical power system testbed, the ADAPT testbed at NASA ARC. The estimates are computed in milliseconds on a PC. The approach performs well despite unmodeled transients and other modeling uncertainties present in the system.

I. PROBLEM

We consider a DC (direct current) electric circuit with sources, loads, and switching elements. Voltage and current measurements are available at certain circuit locations. The problem is to estimate, from the measurements, the fault states of the circuit. The faults are defined as the deviations from the nominal state. The source voltages or loads can differ from their nominal values; voltage and current sensors can be faulty; assumed open/closed states of relays and breakers might differ from their actual states; short-circuit and open-circuit faults are possible, including shorts to the ground. We are interested in the case when several faults might be present simultaneously; however it is known that the fault state is a sparse vector, i.e., most of its components are zero.

Let $y \in \mathbb{R}^{N_m}$ be a vector of observations (measurements). The fault states are described by a vector $f \in \mathbb{R}^{N_f}$. The problem is: given the observations y , estimate faults f . The states of the circuit (e.g., voltages and currents) are described by a vector $x \in \mathbb{R}^{N_s}$ and have to be estimated along with f .

Section III below describes a model of the form

$$0 = Ax + Bf + \xi, \quad (1)$$

$$y = Cx + Df + \eta, \quad (2)$$

where matrices A , B , C , D have appropriate dimensions. The process noise vector $\xi \in \mathbb{R}^{N_s}$ describes the modeling error; the measurement noise $\eta \in \mathbb{R}^{N_m}$ describes the observation error. The state equation (1) and the observation equation (2) are similar to linear state space model commonly used in estimation, except the model (1), (2) is static.

We compute an estimate of the fault vector f and the state x by solving the quadratic programming (QP) optimization problem

$$\text{minimize } \frac{1}{2} \|Ax + Bf\|_Q^2 + \frac{1}{2} \|Cx + Df - y\|_R^2 + \lambda^T |f| \quad (3)$$

where $\|z\|_Q^2 = z^T Q z$; Q , R are positive definite matrices; $|f|$ is the component-wise absolute value; λ is a vector with positive components. The last term provides a weighted l_1 penalty for the unknown components of vector f .

Optimization-based estimation of electrical power systems is well established area, e.g., see [1], [19] for an overview. More discussion is given in Section II. The novelty of the formulation (3) is that the faults f are introduced in a structured way separately from the states x . Another novelty is in use of quadratic penalty for mismatches ξ , η in the model (1), (2), which are usually small; at the same time an l_1 penalty is used for the fault vector f , which is usually large and sparse. We demonstrate that such formulation allows for efficient and accurate estimation of the faults. Additional theoretical justification of the proposed approach can be found in [29].

Problem (3) can be interpreted as Bayesian Maximum A posteriori Probability (MAP) estimation of x and f given y . The MAP formulation assumes Gaussian noises $\xi \sim N(0, Q^{-1})$ and $\eta \sim N(0, R^{-1})$ in (1), (2). A Laplacian prior distribution is assumed for the fault vector f . No prior is assumed for the state x . The noise covariance matrices R and Q in (3) and the fault prior parameters λ can be thought of as parameters that describe the distributions, or as the tuning knobs of the estimation algorithm.

The main benefit of using l_1 regularization in (3) is that for properly selected weights λ the solution vector f is sparse, with many zero components. See [6], [9], [27], [28] for the recent work and further references on sparse solutions using l_1 regularization. The sparsity property matches well the needs of fault estimation and detection. Another advantage of formulation (3) is that linear constraints can easily be added to the problem. Section V considers such constraints describing a prior knowledge of certain voltages and currents being positive.

The proposed optimization-based estimation approach works as follows. At each time step, the observed data are collected into vector y and QP problem (3) is formed. The estimate f is then computed using a QP solver. The QP problem (3) can be solved very fast, in milliseconds for hundreds of states, using modern interior-point methods, see [5]. Because the problem is convex, attaining the global optimum is guaranteed.

This work was supported by the NASA Grant NNX07AEIHA Information Systems Laboratory, Department of Electrical Engineering, Stanford University, Stanford, CA 94305, {gorin,boyd}@stanford.edu
NASA Ames Research Center, Moffet Field, CA 94035, scott.poll@nasa.gov

Today electric utilities use EMS (Energy Management Systems) to monitor, control, and optimize the transmission and generation facilities. Optimization-based estimation is presently used for power systems monitoring, see [19], [1]. On-line QP optimization is also used in Model Predictive Control systems broadly employed in industry, see [24].

II. MOTIVATION

This work was initially motivated by the interest of the aerospace systems community in Integrated Vehicle Health Management (IVHM). IVHM systems collect data from sensors and electronic systems of aircraft (or spacecraft) and diagnose fault conditions or provide predictive warning of incipient faults. Diagnostic estimation for Electric Power Systems (EPS) is important because of trend towards more electric aircraft; wiring problems on aging aircraft (short circuits, arching) are important as well, e.g., see [12], [26].

There is a large body of prior work in diagnostics of electric power systems. Much work is focused on specific electric power system units and elements, such as electric machines, motors, generators, inverters, batteries, solar cells, relays, and other. Work on integrated diagnostics of power distribution systems with many interconnections is primarily focused on AC (alternating current) power distributions systems, e.g., [8]. A few papers consider large vehicle electric systems: integrated diagnostics of international space station is discussed in [11]; diagnostics of marine vehicle power system in [16]; integrated diagnostics and prognostics of aircraft electric system in [12].

The integrated diagnostics architectures in the above cited papers have a degree of commonality. First, there is subsystem-level (unit-level) diagnostics logic, which is often discussed under a name of ‘software agents’. The subsystem-level diagnostics is specific to a particular subsystem type. Second, there is ‘integrated reasoning’ or ‘sensor fusion’ to integrate the subsystem-level diagnostics; typically, AI-type computational reasoning is used.

Our formulation is related to the approaches in optimization-based estimation of power system state that were developing since 1969, see [4], [2] and the books [1], [19] for an overview. The state of AC power system includes the power flows and phase angles in all branches. The state vector is determined by least squares fit of the nonlinear equations relating the state variables and the measurements (e.g., voltage or current magnitudes). The problems are generally nonconvex and an efficient solution with global convergence is difficult to achieve.

Most of the power system estimation work is not oriented towards fault diagnostics. However, a portion of this work explicitly takes into account possibility of outliers in the measurements data (an equivalent of the sensor fault) and unknown states of the circuit breakers (might be caused by a fault). A number of papers discuss using l_1 model fit error instead of the quadratic error for countering and detecting bad measurement data, e.g., [10], [14], also see [2], [4]. The papers [25], [13], [7] look into the problem of determining

network topology errors. In [25], [13] mixed integer problems for determining topology are formulated and different relaxation approaches are pursued. These papers pursue nonconvex optimization problems and use many heuristics. The approach of [7] and several follow-on papers is based on thresholding Lagrange multipliers in the quadratic fit problem with topology-induced constraints.

Recent use of GPS for time synchronization made possible accurate phase measurements and harmonic state estimation of power systems, e.g., see [17]. Harmonic models are linear in quadrature components of voltages and currents, which makes them close to the models in this paper. An approach using l_1 penalty in harmonic source estimation is discussed in [15].

This paper considers a DC power system with linear constitutive equations (1), (2). We show how the fault parameters can be chosen to preserve the linearity, including the topology changing faults. For the convex optimization problem (3) the solution can be obtained in one call to a standard QP solver, without a need for tweaking. Our approach can be extended to fault estimation in harmonic power system analysis, where the equations are linear.

We implement the approach for the ADAPT EPS testbed. This testbed was developed and is maintained at NASA ARC as an experimental platform for research in integrated systems health management, diagnostics, and prognostics. More detail on ADAPT can be found in [23]. Over the last few years ADAPT was used in preliminary studies of diagnostics approaches based on AI-type reasoning and several heuristics, see [3], [18]. These approaches might take from several seconds to many minutes for computing a single diagnosis and have difficulty with diagnosing multiple simultaneous faults. We demonstrate that the proposed optimization-based estimation approach works very well for ADAPT. The solution is computed in milliseconds. We use a static DC model and there might be a concern that the transients in the circuit would cause a problem. Our experimental results show that the transients are not an issue.

In summary, the contributions of this paper are as follows.

- 1) The paper formulates an estimation approach for a DC power system that is specifically aimed at detecting and diagnosing faults and uses a structured fault model. An l_1 penalty is used for the faults and a quadratic penalty is used for other mismatches in the equations. The approach allows modeling of faulty measurements and of faulty circuit topology data. It produces a sparse fault vector estimate.
- 2) The proposed approach is conceptually simple and works reliably. A small number of tuning parameters is required. The implementation is amenable to existing QP solver technology.
- 3) The approach is verified to perform well for multiple faults in extensive simulations.
- 4) The approach is successfully validated in ADAPT testbed experiments and demonstrated suitable for real-time on-line implementation at millisecond timescale.

III. MODEL

This section formulates a linear model of the form (1), (2) for a DC circuit. Section V details an instance of such model for the ADAPT EPS.

We consider a static circuit comprised of current sources (batteries), switching elements, and loads. The available measurements include currents, voltages, and switching element states (open/closed). Ground faults and other short-circuit faults can be included in the model as switching elements that are thought to be open, but could fail into a closed state.

A. State equations

We formulate the Sparse Tableau Analysis (STA) equations of the nodal DC circuit in a standard way, e.g., see [22]. The STA model is sufficiently general and is the core of most standard small-signal linear analysis of electric circuits. This section extends the STA to include a linear model of the faults. We consider several types of faults. Some of them or all of them, might be present and need to be considered.

The circuit has N_N nodes; each node has a voltage e_k with respect to the ground. The circuit contains N_B branches, each has current j_l and voltage drop v_l . The signs of the currents and the voltage drops are relative to the directions of respective branches (graph edges). The incidence matrix $G \in \mathfrak{R}^{N_N, N_B}$ has entries $g_{kl} = 1$ if the branch l leaves the node k , $g_{kl} = -1$ if it enters node k , and $g_{kl} = 0$ otherwise. The STA equations comprise Kirchhoff's Current Law (KCL), Kirchhoff's Voltage Law (KVL), and Branch Constitutive Equations (BCE), which are discussed below.

The KCL equations for the currents $j \in \mathfrak{R}^{N_B}$ can be expressed as

$$S_B G j = 0 \quad (4)$$

where $S_B \in \mathfrak{R}^{N_I, N_N}$ is a selection matrix that un-selects the boundary nodes of the circuit for which KCL does not hold (the current might flow to or from the outside of the modeled circuit).

The KVL relates voltage drops $v \in \mathfrak{R}^{N_B}$ to the node voltages $e \in \mathfrak{R}^{N_N}$

$$G^T e = v \quad (5)$$

Finally, the BCE relate the branch voltage drop and the current as

$$-K_I j + K_V v = f_G \quad (6)$$

where K_V and K_I are diagonal matrices. A diagonal entry of K_V could be conductance; in that case the respective entry of K_I is unity. Alternatively, a diagonal entry of K_I could be a branch resistance; in that case the respective entry of K_V is unity. The components of the fault vector f_G describe the faults in the branches.

For a branch fault, (5) and (4) still hold while (6) would have an error $f_{G,j} = f_{*,j}$. A straightforward relaxation approach is to assume $f_{G,j} = s_j f_{*,j}$, where $s_j = 1$ if the fault is present and $s_j = 0$ otherwise. We could then solve the least square fit problem assuming s_j is a real and adding

a sparsity-inducing l_1 penalty for vector s . It is easy to see that such approach is equivalent to (3).

We consider a few types of faults. The fault of switching element k , which is thought open but might be actually closed is expressed in the form (6) as

$$-j_k = f_{G,k}, \quad (7)$$

where the fault parameter $f_{G,k}$ is a current through the switching element. The current should be zero if the switching element is open.

The fault of a switching element k , which is thought closed can be expressed in the form (6) as

$$v_k = f_{G,k}, \quad (8)$$

where the fault parameter $f_{G,k}$ is a voltage drop at switching element. The voltage drop should be zero if the switching element is closed.

Finally, consider faults of the DC loads. We assume that the load resistance is known. The load fault can be described as the load current being different from what is given by the BCE. The BCE model (6) for branch k with the load fault is

$$g_k v_k - j_k = f_{G,k}, \quad (9)$$

where g_k is the branch conductance and $f_{G,k}$ is a load current deviation from the model, which is indicative of the fault.

B. Observation equations

The STA equations need to be complemented by observation equations. We model sensor faults through additive offsets caused by these faults.

We assume that the observations include the currents $j_{meas} \in \mathfrak{R}^{M_I}$ measured by current sensors and voltages $e_{meas} \in \mathfrak{R}^{M_V}$ measured by voltage sensors. The respective observation equations have the form

$$e_{meas} = S_V e + f_V, \quad (10)$$

$$j_{meas} = S_I j + f_I, \quad (11)$$

where f_V and f_I are fault offsets, S_V and S_I are selection matrices.

We also count the known voltage sources $e_{srce} \in \mathfrak{R}^{M_S}$ and grounded nodes $e_{grnd} \in \mathfrak{R}^{M_G}$ (we assume that $e_{grnd} = 0$) among the observations. Though no on-line voltage sensing might be available for the source voltages, there might be an off-line knowledge of these. The respective observation equations have the form.

$$e_{srce} = S_S e + f_S, \quad (12)$$

$$e_{grnd} = S_G e, \quad (13)$$

where f_S is the fault offset, S_S and S_G are selection matrices. We do not consider ground voltage faults though it would be easy to add these to the model.

The voltage offset f_V , the current offset f_I , and the source (battery voltage) offset f_S are unknown vectors of appropriate dimensions.

C. STA model with faults

To integrate the STA equations, introduce a state vector $x \in \mathfrak{R}^{2N_B+N_N}$ and a matrix $A \in \mathfrak{R}^{2N_B+N_{in}, 2N_B+N_N}$ as

$$x = \begin{bmatrix} j \\ v \\ e \end{bmatrix}, \quad A = \begin{bmatrix} S_B G & 0 & 0 \\ 0 & I & -G^T \\ K_I & K_V & 0 \end{bmatrix}, \quad (14)$$

Let f be a vector of all fault parameters.

$$f = [f_G^T \ f_V^T \ f_I^T \ f_S^T]^T \in \mathfrak{R}^{N_F}, \quad (15)$$

where $N_F = N_B + M_V + M_I + M_S$. Introduce the observation vector $y \in \mathfrak{R}^{M_y}$, where $M_y = M_I + M_V + M_S + M_G$, and the observation matrix $C \in \mathfrak{R}^{M_y, 2N_B+N_N}$. The combined observations can be expressed as

$$y = \begin{bmatrix} j_{meas} \\ e_{meas} \\ e_{srce} \\ e_{grnd} \end{bmatrix}, \quad C = \begin{bmatrix} S_I & 0 & 0 \\ 0 & 0 & S_V \\ 0 & 0 & S_S \\ 0 & 0 & S_G \end{bmatrix}, \quad (16)$$

Introduce matrix $B \in \mathfrak{R}^{2N_B+N_{in}, N_F}$ describing the fault impact on the states x and matrix $D \in \mathfrak{R}^{N_y, N_F}$ describing the impact of the sensor faults on the observation vector y

$$B = \begin{bmatrix} 0 & 0 & 0 & 0 \\ 0 & 0 & 0 & 0 \\ B_G & 0 & 0 & 0 \end{bmatrix}, \quad D = \begin{bmatrix} 0 & B_I & 0 & 0 \\ 0 & 0 & B_V & 0 \\ 0 & 0 & 0 & B_S \end{bmatrix}, \quad (17)$$

The faults enter equations linearly. After pulling together state equations (4), (5), (6) and observation equations (10), (11), (12), and (6) and adding noises ξ and η we obtain the linear model of the form (1), (2). In this model x , y , A , and C are given by (14), (16); the faults are defined by (15) and the fault-related matrices B , D in (1), (2) have the form (17).

For zero noises $\xi = 0$, $\eta = 0$ the STA equations (1), (2) make a system of total $M_y + 2N_B + N_{in}$ equations in the $2N_B + N_N$ unknown components of vector x . In a special case of $M_y = N_N - N_{in}$ (where $N_N - N_{in}$ is the number of the edge nodes), the system is square and a unique solution can be found. This paper considers the redundant observation case of $M_y \geq N_N - N_{in}$.

IV. VERIFICATION

This section presents an application to ADAPT. We first describe a model of the testbed, then discuss results of simulation based on the model. Next section presents the experimental results.

A. Modeling

We are considering the part of the ADAPT testbed shown in Figure 1, see [23]. The battery voltages V_1 and V_2 are assumed to be known (they are included with the components of the observation vector y). There are six branch resistances (loads) that are assumed to be known as well: these include two internal resistances of the batteries RB1, RB2; two DC load resistances RDC1, RDC2; and two equivalent resistances RAC1, RAC2, of the AC load branches (including the AC/DC inverters). The resistances of the circuit breakers and relays are assumed to be zero in the closed state and infinity

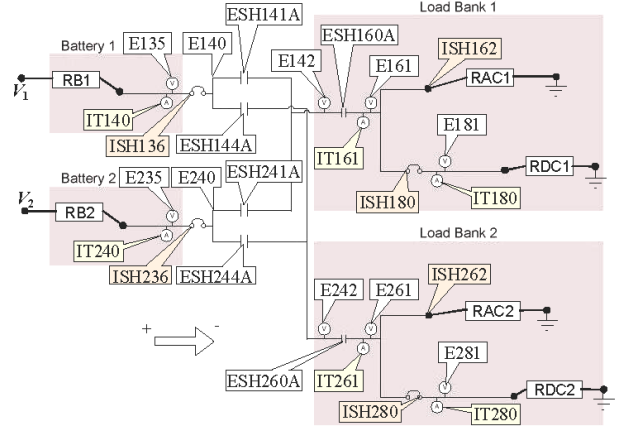


Fig. 1. Data tags for the ADAPT circuit

V_1	V_2	RBAT1	RBAT2	RAC1	RDC1	RAC2	RDC2
25.84	24.83	0.1	0.1	6	10	4	20

TABLE I
ADAPT SIMULATION PARAMETERS

in the open state. The circuit parameters were identified from experimental data.

As illustrated in Figure 1, there are a total of six current sensors in the circuit, which correspond to the components of the current measurement vector j_{meas} in (11). There are a total of ten voltage sensors corresponding to the components of the voltage measurement vector e_{meas} in (10)

The branch constitutive equations (6) are defined by the states of the switching elements (six relays and six circuit breakers). These states indicating whether the switching element is open or closed are collected from the embedded switching element sensors in ADAPT.

B. Simulation

The incidence matrix of the circuit was defined in accordance with Figure 1. The circuit parameters (source voltages and resistances) used in the simulation are summarized in Table I. The notation is the same as in Figure 1.

The simulations used the STA model (1), (2), (14), (16), (15), (17) with zero noises ξ and η . In the simulations, the model matrices were formed as described above, with the following variation. The current and voltage measurements were ignored by assuming $M_I = 0$, $M_V = 0$, and eliminating the vectors j_{meas} , e_{meas} , from the observation equations (11), (10). The resulting system of equations has $2N_B + N_N = 54$ states x and $2N_B + N_{in} + M_S + M_G = 54$ equations, where $N_B = 18$, $N_N = 18$, $N_{in} = 12$, $M_S = 2$, and $M_G = 4$. The M_S source voltages and M_G ground voltages (6 at all) define $N_N - N_{in} = 6$ boundary conditions. For given switching

ESH141A	ESH144A	ESH160A	ESH241A	ESH244A	ESH260A
open	open	closed	closed	closed	closed

TABLE II
BASIC RELAY CONFIGURATION IN THE SIMULATION

element states, the resulting square system was solved to determine the state vector x .

The switching element states define the BCE matrices K_I and K_V in (6), (14). The basic switching element configuration in the simulation is shown in Table II. All breakers are assumed closed. The relays are configured to connect Battery 2 to all DC and AC loads; Battery 1 is disconnected from the loads.

The simulation input is the fault state f , which we generated as a sparse random vector. The simulation output includes the original switching element states, (before the applied faults), and the sensor measurements (computed after applying the faults). The switching element faults were applied by inverting the respective open/closed states before calculating the BCE matrices K_I , K_V , and the STA matrix A (14) in accordance with (7), (8).

The load faults were applied by modifying the respective load resistances in BCE (6). The resistances shown in Table I were modified by a given percentage in the range from -50% (-100% corresponds to a short circuit) to +50%. The source faults were applied by modifying the the respective value of e_{src} in (16). The source voltages shown in Table I were modified by a given percentage in the range from -50% (-100% corresponds to zero battery voltage) to zero (no change in the voltage).

The current sensor measurements and the voltage sensor measurements at the simulation output were modified by adding offsets proportional to the respective fault magnitudes. The fault offsets for current sensors were distributed in the range from -1A to 1A. The fault offsets for the voltage sensors were distributed in the range from -12V to 12V.

In the simulations, all parametric faults were constrained to be at least 20% of the respective maximum magnitude. This avoids small faults that are below the noise level.

C. Diagnostics of simulated data

The diagnostics algorithm uses model (1), (2). The main differences with the simulation model are as follows.

- The diagnostics model includes faults. The fault model is described by (15), (17).
- In the diagnostics model, the switching elements are assumed to be in the nominal state. If a fault is present, the actual state differs from the nominal.
- The observations (2), (16) in the diagnostic model are the currents and the voltages distorted by noise η .
- The observation and process noises ξ and η in the diagnostic model (1), (2) are described through the inverse covariance matrices R and Q .

The fault estimation algorithm is implemented in Matlab. The dimension of fault vector f (15) is $N_F = N_B + M_V + M_I + M_S = 38$. The fault estimates were computed by solving QP problem (3) and then thresholding the absolute values of the fault vector f . The tuning parameters are chosen as follows. All variables were made nondimensional: the currents were divided by a scaling parameter 3 A, the voltages, by the scaling parameter 10 V. The noise inverse covariance matrices Q and R were set up by multiplying

- 1) Battery 1 circuit breaker ISH136 (BATT 1 CB) thought closed fails open. This fault is misdiagnosed for an offset of BATT 1 voltage sensor E135. The reason is that no current is flowing through BATT 1 CB; the relays are open and an open CB disconnects Branch 1. Floating voltage of the sensor E135 floats is the only observed indication of the fault.
- 2) DC/AC Inverter 1 (INV 1) input CB thought closed fails open. This fault is misdiagnosed for an offset of INV 1 load current. The diagnosis confuses the faults of the current sensor and CB; both change inverter load current. The faulty part of the circuit is pointed out correctly.
- 3) DC/AC Inverter 2 (INV 2) input CB thought closed fails open. This fault is mis-diagnosed for an offset of INV 2 load current. Same comment as 2.
- 4) EY141A relay thought open fails closed. This fault is mis-diagnosed for three faults: offset of BATT 1 output current sensor, two relays EY141A and EY144A thought open fail closed. The actual fault is detected correctly; in addition to that, there are false positives. The change in the current balance could be attributed to each of the diagnosed faults.
- 5) BATT 1 CB output voltage is offset. The actual fault is detected correctly, but there is false positive: EY136 CB thought closed is misdiagnosed failing open. No current flows through the CB and it failing open cannot be excluded based on the data observed. See # 1 for more explanation.

TABLE III
SINGLE FAULT DIAGNOSTICS ERRORS

unity matrices of respective size by the weight of 100; this corresponds to assuming a standard deviation 0.1 for the noises. The fault covariance matrix Λ was set to a unity matrix times 2. The thresholds for detecting the faults were set to 0.05, except the 0.2 threshold for detecting switching element faults.

The problem (3) is transformed into a standard form of a QP problem by substituting $f = f_+ - f_-$, where $f_+ \geq 0$, $f_- \geq 0$. The decision variables include the vectors x of dimension $2N_B + N_N = 54$ and vectors f_+ , f_- of dimension 38 each. There are 130 decision variables at all. The QP problem was solved using Mosek, see [20]. The solution takes about 20 msec on a 2 Ghz Wintel laptop computer. This is suitable for real-time implementation and much faster than 0.5 sec sampling time for ADAPT data collection.

In the simulation experiments, a series of fault patterns were seeded (input into the simulation) to generate the sensor data. The estimation algorithms are applied to the simulated sensor data and the diagnosis of the fault state is compared to the seeded faults. In great majority of the simulation runs, the estimation algorithms diagnose the seeded faults exactly. We will focus on the cases when the diagnosis was inexact.

The first series of tests was to seed all faults, one fault at a time. There were 5 imperfect diagnoses encountered among the 38 total cases, one case for each fault component. While imperfect, these diagnoses were not, strictly speaking, incorrect. They can be explained by examining the circuit diagram in Figure 1. The imperfect diagnoses are discussed in Table III.

The second series of tests was to seed two faults at a time. (In each test, all but two components of vector f were zeros). In a majority of cases, a perfect diagnosis was achieved. Each time one of the five single faults from Table III was

- 1) EY160A relay thought closed fails open and EY236 CB thought closed fails open. EY236 CB failing open is the only fault diagnosed. EY236 CB failing open disconnects the battery and powers down the rest of the circuit; this makes the rest of the diagnostics ineffective. Many more cases like that were encountered.
- 2) E242 voltage sensor is offset and EY244A relay thought closed fails open. EY244A relay failing open is diagnosed correctly, the second fault is misdiagnosed for EY260A relay thought closed failing open. Open EY244A relay disconnects the load. This is similar to Case # 1 above. The failures in an unpowered branch can not be diagnosed correctly.
- 3) EY241A relay thought closed fails open and load resistance is offset. Only the first fault is diagnosed. Again, the failures in the unpowered branch are not observable.
- 4) EY141A and EY241A relays thought open fail closed. EY141A relay thought open failing open is diagnosed correctly, the second fault is misdiagnosed for EY144A relay thought open failing closed. Nominally, BATT 2 should be connected while BATT 1 is disconnected. The diagnosis that the fault causes BATT 1 to connect is correct. The fact that BATT 2 is disconnected and the states of relays and breakers are diagnosed imprecisely. This is because the parallel connection of the batteries makes the currents through them very sensitive to the (close) battery voltages and (small) internal resistances.
- 5) Resistances of the two DC loads are offset. Only offset on DC 1 Load is diagnosed. The fault is below the threshold. As Table I, shows, the undetected DC Load 2 has the highest resistance (the least power) of all the loads. Increasing the threshold, or decreasing the l_1 regularization penalty Λ makes the diagnostics more sensitive and could allow to detect this fault. At the same time, more false positives will be generated.

TABLE IV
TWO-FAULT DIAGNOSTICS ERRORS

encountered, the diagnosis was imperfect as explained above. Besides the expected imperfections of diagnostics caused by the single faults from Table III, combinations of two faults introduce new ways for the diagnostic algorithm to be in error.

About 200 two-fault cases were randomly generated out of the entire set of the $38 \cdot 37/2 = 703$ double fault cases. The results were manually examined and are instructive. The cases of the diagnostic algorithm not working perfectly are discussed in Table IV. While imperfect, most of these diagnoses are not incorrect.

In summary, the proposed approach works quite well in simulation. In a majority of the cases the diagnosis is perfect. In the great majority of all cases, the problematic circuit branch is diagnosed correctly. The remaining imperfect diagnoses make for less than 5% of all cases and are caused by high or low problem sensitivities to some of the fault parameters.

The ADAPT circuit includes DC/AC inverters and AC loads. The inverter together with the AC load circuit can be modeled through an equivalent DC resistance. A linearized model can be fitted into a number of observations of the steady state inverter draw currents and the inverter supply voltages for the given load. A suitability of such simplified inverter model is confirmed by the experimental results.

V. VALIDATION

The ADAPT testbed is an instrumented EPS with two sets of computer controls. The data from the first set are

called ‘‘Observer’’ data and are used for testing diagnostic algorithms. These data were used in this work. The second, independent set of controls, known as ‘‘Antagonist’’ is employed in creating fault conditions for the Observer. These controlled fault conditions are known and used as a reference when evaluating diagnostic method performance. More detail on ADAPT can be found in [23].

Once verified in the simulation, the algorithms were integrated with ADAPT and validated in experiments.

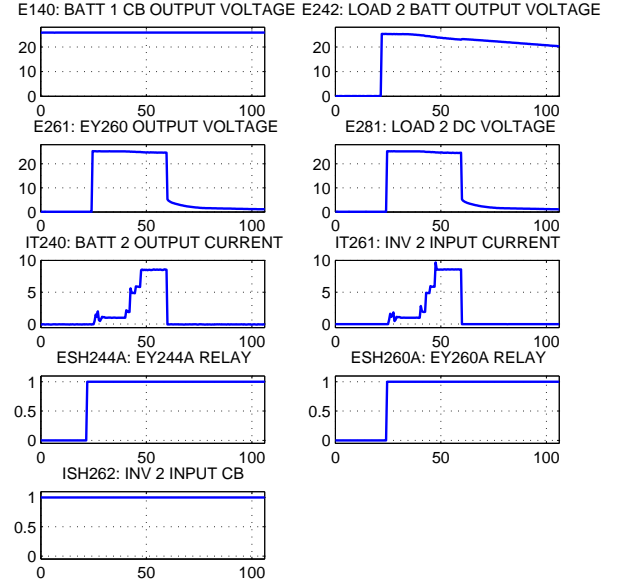


Fig. 2. Observed experimental data

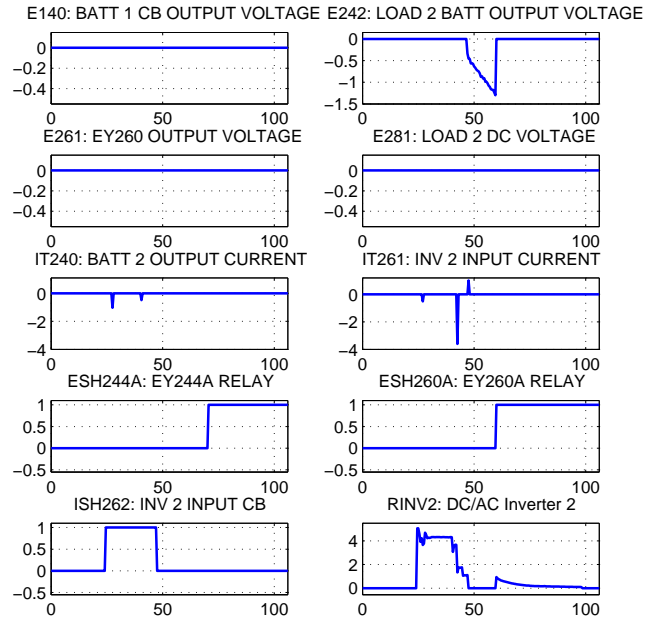


Fig. 3. Estimated fault states for the experimental data

One data set used for the algorithm testing is displayed in Figure 2. The data was collected at 2 Hz rate (0.5 sec

interval). In the experiment, all loads are initially unpowered. Then relays EY244A and EY260A close to connect Battery 2 and to power AC Load 2. After a transient, the DC/AC Inverter 2 powers the AC load nominally. After several seconds, relay EY260A fails (opens). This disconnects the load. The faulty relay sensor continues to show that the relay is closed. The described scenario is complemented by a voltage sensor fault (offset ramp). Figure 2 shows 9 plots of selected observed signals, those with a transient and those later found faulty. The remaining 27 channels out of the 36 monitored show constant values, e.g., battery voltages or circuit breaker states (all closed) and are not plotted.

When applying the diagnostic algorithms to the data, the model parameters were set as follows. The source voltages were determined from the initial data segment with no current flow through the batteries. The voltages are $V_{BAT1}=25.84$ V and $V_{BAT2}=24.83$ V. The DC/AC Inverter 2 load model was determined from the data segment corresponding to nominal steady state operation of the load as $R_{INV2}=2.8871$ Ohm.

Though the data contains transients, the diagnostic algorithm assume a steady state model at each step. The steady-state model used for diagnosis neglects the transients. Despite that, the algorithms are able to detect and diagnose the seeded faults. The results are illustrated in Figure 3, which shows the fault estimates corresponding to the signals in Figure 2. The diagnosis was imperfect during the inverter transient (which was diagnosed as a fault) in the circuit branch that became unpowered. The reason for large deviation transient in the inverter current is that the model assumes a steady-state condition in which all of the loads in load bank 2 are on after EY260 is closed. However, at the start of the inverter transient at 27.5 seconds, the inverter takes approximately 6 seconds before power appears at the output. Then, it takes an additional 14 seconds before all the loads are turned on and the equivalent resistance reaches the full RAC2 value that is used in the model.

The lower right plot shows an estimate of the fault current (deviation from the nominal current) for the DC/AC Inverter 2 with the AC load. Switching of the relays and inverter excites very large current transients. These causes false positives for current sensor faults. The middle plots in Figure 3 show three false positive occurrences for one sensor and two for another, one time-sample duration each. The timeline of the events and the diagnostic estimation results with a commentary are detailed in Table V.

VI. CONCLUSIONS

Overall, the discussed diagnostics approach works very well for the DC power system applications exemplified by ADAPT. The diagnosis is accurate when this can be expected. The diagnostic algorithm uses a straightforward nodal DC circuit model with a minimum of detail. The algorithm has a few well-defined parameters that need to be set up and takes milliseconds to compute results. The approach has been demonstrated to work well with ADAPT experimental data despite ignoring the transients and modeling a complex

Time: Event	Description
t=24: Control action	Relays EY244A and EY260A are closed to power the load
t=27.5: Start of INV2 transient	INV2 Input CD ISH262 is suspected open; INV2 Load is suspected to be off-nominal
t=34: Sensor fault occurs	E242 voltage offset starts ramping down from zero
t=46.5: Sensor fault detected	E242 voltage offset is detected during the inverter transient
t=47.5: Nominal regime	Inverter reaches a steady state
t=59.5: Relay fault occurs	Relay EY260A opens and cuts off the branch with the DC/AC inverter load and E242 voltage sensor
t=60: Relay fault detected; sensor fault goes undetected	Relay EY260A failure is detected; E242 voltage offset fault in the cut-off branch stops being detected
t=65.5: Relay fault detected, sensor fault undetected, false detection of a second relay fault	The large offset of voltage measurement E242 is now interpreted as a voltage across relay EY244A in the disabled branch indicating that the relay failed open.

TABLE V

TIMELINE OF EVENTS IN EXPERIMENTAL DATA AND FAULT ESTIMATION

circuit of DC/AC inverter with a load by a single DC resistor. The approach might briefly mistake some of the transients for the faults, but location of such false positives is correctly attributed to the source of the transients. The approach is clearly suitable for on-line implementation in practical monitoring or diagnostic systems.

REFERENCES

- [1] A. Abur and A. Gomez Exposito, *Power System State Estimation: Theory and Implementation*, New York, NY: Marcel Dekker, 2004.
- [2] M.E. Baran and A. Abur, "Power System State Estimation," in J. Webster (ed.), *Wiley Encyclopedia of Electrical and Electronics Engineering*, 1999 John Wiley and Sons, Inc.
- [3] M. Daigle, X. Koutsoukos, and G. Biswas, "An Event-based Approach to Integrated Parametric and Discrete Fault Diagnosis in Hybrid Systems," *Trans. Inst. of Measurement and Control*, Special Issue on Hybrid and Switched Systems, to appear.
- [4] A. Bose and K.A. Clements, "Real time modeling of power networks," *Proc. IEEE*, Vol. 75, No. 12, pp. 1607-1622, 1987.
- [5] S. Boyd and L. Vandenberghe, *Convex Optimization*, Cambridge University Press, 2004.
- [6] E. J. Candes, J. Romberg, and T. Tao. "Stable signal recovery from incomplete and inaccurate measurements," *Communications on Pure and Applied Mathematics*, Vol. 59, 2006, pp. 1207-1223.
- [7] K.A. Clements and A.S. Costa "Topology error identification using normalized Lagrange multipliers", *IEEE Trans. on Power Systems*, Vol. 13, No. 2, pp. 347-353, 1998.
- [8] E.M. Davidson, S.D.J. McArthur, J.R. McDonald, "A toolset for applying model-based reasoning techniques to diagnostics for power systems protection," *IEEE Trans. on Power Systems* Vol. 18, No. 2, 2003, pp. 680-687.
- [9] D. Donoho, "Compressed sensing," *IEEE Transactions on Information Theory*, Vol. 52, No 4, 2006, pp. 1289-1306.
- [10] M.R. Irving, R.C. Owen, and M.J.H. Sterling, "Power System State Estimation Using Linear Programming," *Proc. IEE.*, Vol. 125, pp. 879-885, 1978.
- [11] A. Gonzalez, R. Morris, F. McKenzie, D. Carreira, B. Gann, "Model-based, realtime control of electrical power systems," *IEEE Trans. on Systems, Man, and Cybernetics*, Vol. 26, No. 4. 1996, pp. 470-482
- [12] K. Keller, K. Swearingen, J. Sheahan, M. Bailey, J. Dunsdon, K.W. Przytula, B. Jordan, "Aircraft electrical power systems prognostics and health management," *IEEE Aerospace Conf.*, March 2006, Big Sky, MT.
- [13] G. N. Korres and P. J. Katsikas, "Identification of Circuit Breaker Statuses in WLS State Estimator," *IEEE Trans. on Power Systems*, Vol. 17, No. 3, pp. 818-825, 2002.

- [14] W.W. Kotiuga and M. Vidyasagar, "Bad data rejection properties of weighted least absolute value techniques applied to static state estimation," *IEEE Trans. Power Appar. Syst.*, Vol. PAS-101, pp. 844–851, 1982.
- [15] H. Liao "Power System Harmonic State Estimation and Observability Analysis via Sparsity Maximization," *IEEE Trans. on Power Systems*, Vol. 22, No. 1, pp. 15-23, 2007.
- [16] L. Li, K.P. Logan, D.A. Cartes, S.K.Srivastava, "Fault detection, diagnostics, and prognostics: software agent solutions," *IEEE Transactions on Vehicular Technology*, Vol. 56, No. 4, July 2007, pp. 1613–1622.
- [17] A. P. Sakis Meliopoulos, F. Zhang, and S. Zelingher, "Power system harmonic state estimation," *IEEE Trans. an Power Delivery*, Vol. 9, pp. 1701-1709, 1994.
- [18] O.J. Mengshoel, A. Darwiche, K. Cascio, M. Chavira, S. Poll, and S. Uckun, "Diagnosing Faults in Electrical Power Systems of Spacecraft and Aircraft," *20th Innovative Applications of Artificial Intelligence Conference (IAAI-08)*, July 2008, Chicago, IL.
- [19] A. Monticelli, *State Estimation In Electric Power Systems: A Generalized Approach*, Boston: Kluwer, 1999.
- [20] MOSEK ApS, *The MOSEK Optimization Tools Version 5.0. Optimization Tool Manual.*, 2007. Available: www.mosek.com.
- [21] F. Muzi and G. Sacerdoti, "A numerical approach to the diagnostics of electrical distribution networks," *IEEE Power Engineering Society General Meeting*, June 2007
- [22] L.T. Pillage, R.A. Rohrer, C. Visweswarian, *Electronic Circuit and System Simulation Methods (SRE)*, McGrawHill, 1998
- [23] S. Poll, A. Patterson-Hine, J. Camisa, D. Garcia, et al. "Advanced Diagnostics and Prognostics Testbed", *18th International Workshop on Principles of Diagnosis*, pp. 178–185, May 2007.
- [24] S.J. Qin and T.A. Badgewell "An overview of industrial model predictive control technology," *In Chemical Process Control - V*, volume 93, no. 316, pages 232–256, AIChE Symposium Series - American Institute of Chemical Engineers, 1997
- [25] H. Singh and F.L. Alvarado "Network Topology Determination using Least Absolute Value State Estimation," *IEEE Trans. on Power Systems*, Vol. 10, No. 3, pp. 1159-1165, 1995
- [26] R. Spyker, D.L. Schweickart, J.C. Horwath, L.C. Walko, D. Grosjean, "An evaluation of diagnostic techniques relevant to arcing fault current interrupters for direct current power systems in future aircraft," *Electrical Insulation Conference and Electrical Manufacturing Expo*, pages 146-150, Oct. 2005.
- [27] R. Tibshirani. "Regression shrinkage and selection via the lasso," *Journal of the Royal Statistical Society. Series B (Methodological)*, Vol. 58, No. 1, 1996, pp. 267–288.
- [28] J. Tropp, "Just relax: convex programming methods for identifying sparse signals in noise," *IEEE Transactions on Information Theory*, Vol. 52, No 3, 2006, pp. 1030–1051.
- [29] A. Zymnis, S. Boyd, and D. Gorinevsky "Resistor circuit fault detection;" Manuscript, Information Systems Laboratory, Stanford University, 2008 (in preparation)